DEVELOPMENT OF PLASTIC ETA FACTORS FOR DEEP AND SHALLOW CRACKED BEND SPECIMENS EMPLOYED IN *J-R* CURVE TESTING

Sebastian Cravero
Fracture Mechanics and Structural Integrity Group - NVFRAC
Dept. of Naval Architecture and Ocean Eng., University of São Paulo
e-mail: sebastian.cravero@poli.usp.br

Claudio Ruggieri
Fracture Mechanics and Structural Integrity Group - NVFRAC
Dept. of Naval Architecture and Ocean Eng., University of São Paulo
e-mail: claudio.ruggieri@poli.usp.br

Abstract. *The stable tearing of a macroscopic crack in ductile materials for structural applications is conventionally characterized by crack growth resistance (J-R) curves. Under sustained ductile tearing of the (macroscopic) crack-like defect, large increases in the load-carrying capacity of the structure, as characterized by resistance curves, are possible beyond the limits given by the crack driving force at the onset of crack growth. However, structural defects are very often surface cracks that form during fabrication or during in-service operation. These crack configurations generally develop low levels of crack-tip stress triaxiality (crack-tip constraint) which contrasts sharply to conditions present in deeply cracked specimens thereby yielding low resistance curves and increased toughness properties. The above arguments have prompted research efforts to adopt the use of geometry dependent crack growth resistance curves so that crack-tip constraint in the test specimen closely matches the crack-tip constraint for the structural component. However, current standardized methods to determine crack growth resistance properties based upon unloading compliance procedures employing a single specimen, such as ASTM E1820, utilize only bend-type specimens with deep cracks (crack size to specimen width ratios, a/W > 0.5), such as the C(T) and SE(B) specimens. The compliance equations developed for these crack configuration do not necessarily apply to shallow crack specimens. Consequently, new compliance functions are needed to determine crack growth resistance properties using test specimens with small a/W ratios. This work presents the development of compliance equations and solutions of plastic η-factors to evaluate crack growth and J Integral for shallow crack bend specimens. Very detailed linear and non-linear finite element analyses for plane-strain models provide the evolution of load with increased load-line displacement and crack mouth opening displacement which are needed to determine the compliance functions.*

Keywords: *fracture mechanics, compliance, η-factor, J-R curves, ductile tearing*

1. Introduction

The stable tearing of a macroscopic crack in ductile materials for structural applications is conventionally characterized by crack growth resistance (*J-R*) curves. Under sustained ductile tearing of the (macroscopic) crack-like defect, large increases in the load-carrying capacity of the structure, as characterized by resistance curves, are possible beyond the limits given by the crack driving force at the onset of crack growth. Standardized procedures for *J-R* curve testing require both sufficient specimen thickness to insure predominantly plane strain conditions at the crack-tip and deep cracks (crack size to specimen width ratios, $a/W > 0.5$) (ASTM E1152, 1995-ASTM E1820, 2001). Within certain limits on load levels and crack growth, these restrictions insure high levels of stress triaxiality at the crack tip. Since structural defects in common civil and marine strucutres are very often surface cracks that form during fabrication or during in-service operation, the applied driving force needed to the crack grow in laboratory specimens is lower than yhe corresponding drivung force in the structural component. These crack configurations generally develop low levels of crack-tip stress triaxiality (crack-tip constraint) which contrasts sharply to conditions present in deeply cracked specimens thereby yielding low resistance curves and increased toughness properties

The above arguments have prompted research efforts to adopt the use of geometry dependent crack growth resistance curves so that crack-tip constraint in the test specimen closely matches the crack-tip constraint for the structural component. However, current standardized methods to determine crack growth resistance properties based upon unloading compliance procedures employing a single specimen, such as ASTM E1152 (1995) or ASTM E1820 (2001), utilize only bend-type specimens with deep cracks (crack size to specimen width ratios, $a/W > 0.5$), such as the C(T) and SE(B) specimens. The compliance equations developed for these crack configuration do not necessarily apply to shallow crack specimens with much lower crack-tip constraint. Consequently, new compliance functions are needed to determine crack growth resistance properties using test specimens with small a/W ratios.

This work presents the development of compliance equations for evaluation of the *J* Integral and crack growth for shallow cracked bend specimens. The primary objective is to derive plastic η-factors which are applicable to determine *J-R* curves for a wide range of a/W-ratios and material flow properties. Very detailed linear and non-linear finite element analyses for plane-strain models provide the evolution of load with increased load-line displacement (*LLD*) and crack mouth opening displacement (*CMOD*) which are needed to determine the compliance functions. The present results, when

taken together with previous studies, provide a fairly extensive body of results which serve to evaluate crack growth resistance properties using bend specimens with varying geometries.

2. Finite Element Models

Linear and nonlinear finite element analyses are performed on plane-strain models for 1-T SE(B) fracture specimens (which have thickness B=25.4 mm - see fracture testing terminology standardized by ASTM E1823, (2002)). The analysis matrix covers a wide range of three point bend specimens with varying crack sizes to specimen width ratios (a/W = 0.10 to 0.50 with increments of 0.05). Here, a is the crack size and W is the specimen width. All fracture specimens have conventional geometry, i.e., $W = 2B$. Figure 1 shows the geometry and specimen dimensions for the SE(B) specimens.

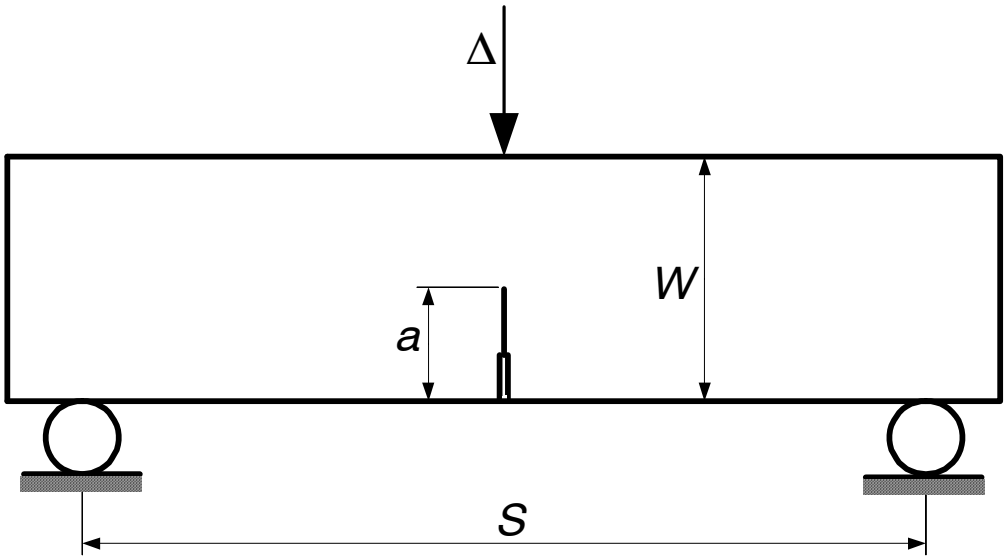

Figure 1. Geometry and dimensions for the analyzed fracture specimen.

The elastic-plastic constitutive model employed in the nonlinear analyses follows a J_2 flow theory with conventional Mises plasticity in small geometry change (*SGC*) setting. The numerical solutions for the fracture specimens utilize a simple power-hardening model to characterize the uniaxial true stress-logarithmic strain. These finite element analyses consider material flow properties covering typical structural steels: n = 5 (E/σ_0 = 800), 10 (E/σ_0= 500) and 20 (E/σ_0=300) with E = 206 *GPa* and ν=0.3; these ranges of properties also reflect the upward trend in yield stress with the decreasing strain hardening exponent characteristic of ferritic steels.

Figure 2 shows the finite element models constructed for the plane-strain analyses of the bend specimens with a/W = 0.20 and a/W = 0.50. All other crack models have very similar features. A conventional mesh configuration having a focused ring of elements surrounding the crack front is used with a small initial root radius at the crack tip (blunt tip) to enhance convergence of the nonlinear iterations as presented in Fig. 2(c); the radius of the blunt tip, ϱ, is 2.5 μm (0.0025 mm). Symmetry conditions permit modeling of only one-half of the specimen with appropriate constraints imposed on the remaining ligament. The half-symmetric model has one thickness layer of 1257 8-node, 3-D elements (2714 nodes) for the a/W = 0.2 and 1225 8-node, 3-D elements (2642 nodes) for the a/W = 0.5 with plane-strain constraints imposed on each node. These finite element models are loaded by displacement increments imposed on the loading points to enhance numerical convergence. The numerical computations for the fracture specimens reported here are generated using the research code WARP3D (Koppenhoefer et. al., 1994).

The mechanical energy release rate at a point along a crack front is given by (see Moran and Shih, 1987)

$$J = \int_{\Gamma} \left[\mathcal{W} n_1 - P_{ji} \frac{\partial u_i}{\partial X_1} n_j \right] d\Gamma \tag{1}$$

where Γ denotes a contour defined in a plane normal to the front on the undeformed configuration beginning at the bottom crack face and ending on the top face, n_j is the outward normal to Γ, $\mathcal{W}$ denotes the stress-work density per unit of undeformed volume, P_{ij} and u_i are Cartesian components of stress and displacement in the crack front coordinate system. The finite element computations employ a domain integral procedure (Moran and Shih, 1987) for numerical evaluation of Eq. (1) computed over domains defined outside material having the highly non-proportional histories of the near-tip fields. Such J-values thus retain a strong domain (path) independence.

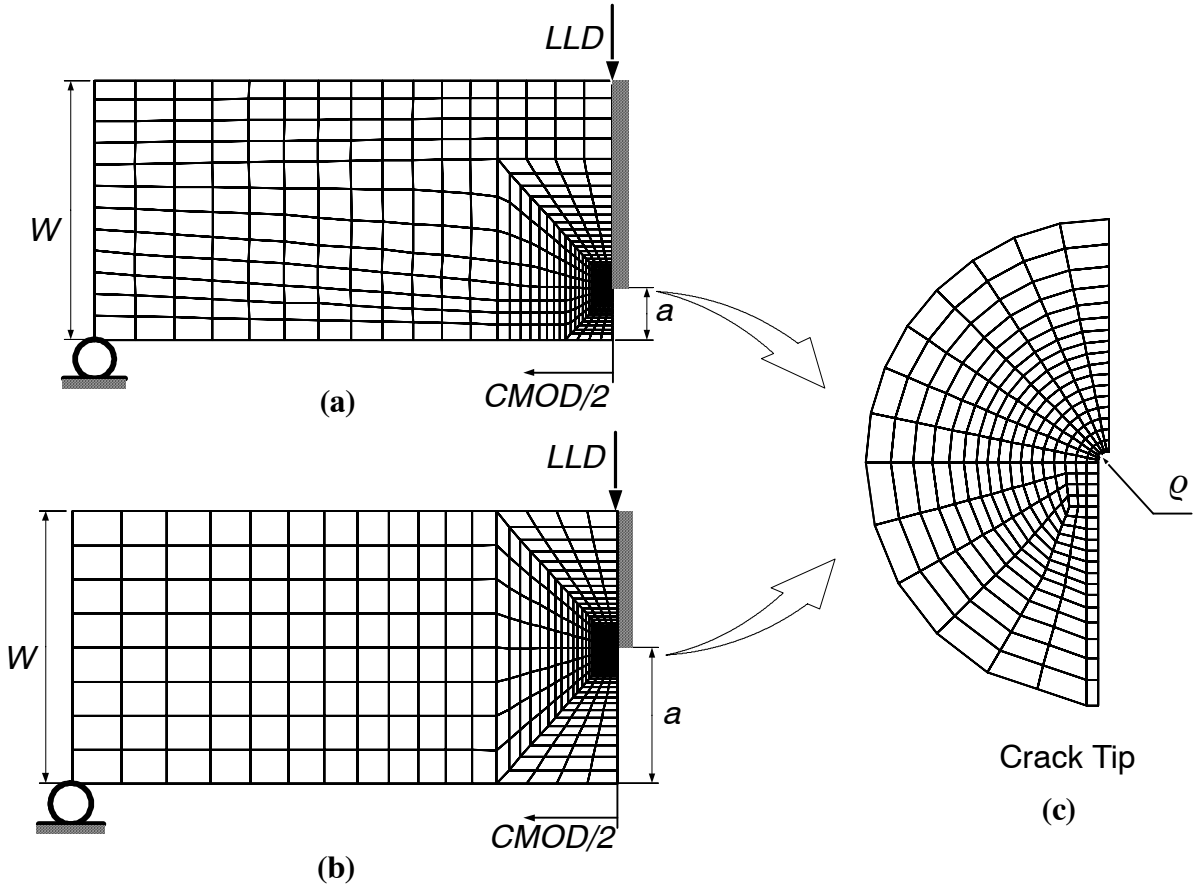

Figure 2. Plane-strain finite element models used in the analyses: (a) 1-T SE(B) specimen with a/W = 0.2; (b) 1-T SE(B) specimen with a/W = 0.5. (c) Near-tip mesh.

3. Compliance Equation

The linear elastic finite elements analyses provide load and *CMOD* records to evaluate the compliance for different a/W ratios. For each specimen with a particular crack size to specimen width (a/W) ratio, the evolution of load against *CMOD* relation gives a straight line with slope equal to the inverse of the compliance. Figure 3 shows the load against *CMOD* curve for a linear elastic analysis of a SE(B) specimen with a/W=0.3. It can be observed in this figure the corresponding compliance for this a/W ratio. By doing the same procedure for different a/W ratios and with a reverse fit using a standard fifth order polynomial the next relation between compliance and crack sizes to specimen width ratio is found

$$\frac{a}{W} = 0.7590 + 1.2961 \cdot u - 37.9076 \cdot u^2 + 154.9671 \cdot u^3 - 270.3815 \cdot u^4 + 182.6632 \cdot u^5 \qquad (2)$$

where

$u = \dfrac{1}{\left(\dfrac{BWEC}{S/4}\right)^{1/2} + 1}$; Normalized Displacement

$C = \Delta v / \Delta P$; Measured Compliance

$v = CMOD$; Crack Mouth Opening Displacement

B : Effective Specimen Thicckness.

Figure 4 compares Eq. (2) with the compliance equation from ASTM E1820 (2001). It can be observed that both equations are similar for crack size to specimen width ratios greater than 0.25 (a/W > 0.25). In contrast, these equations differ markedly for crack sizes to specimen width ratios lower than 0.25.

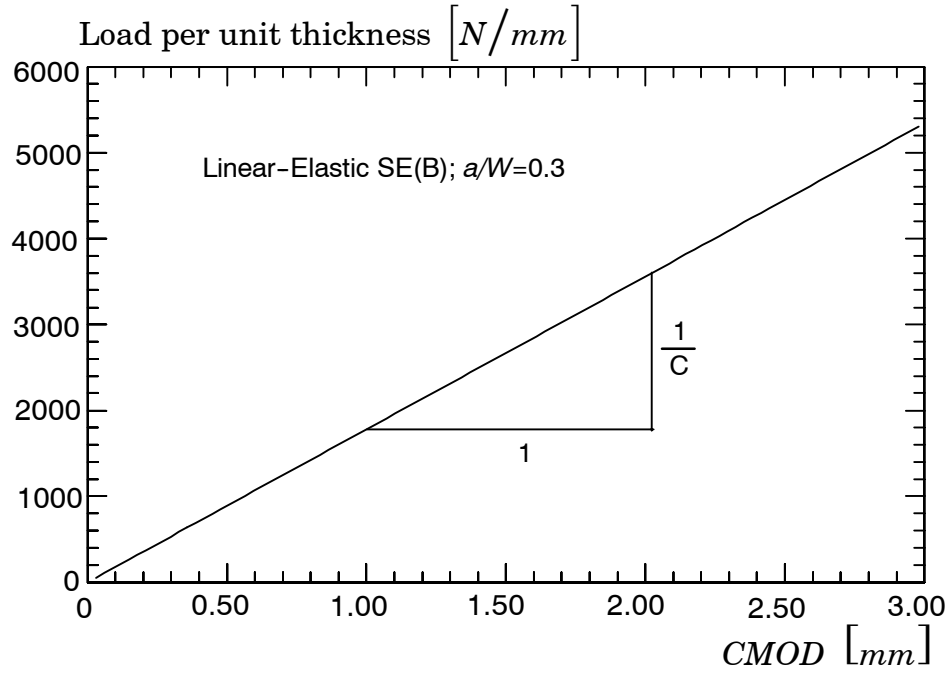

Figure 3. Load vs. *CMOD* for a linear-elastic analysis of a SE(B) specimen with a/W=0.3.

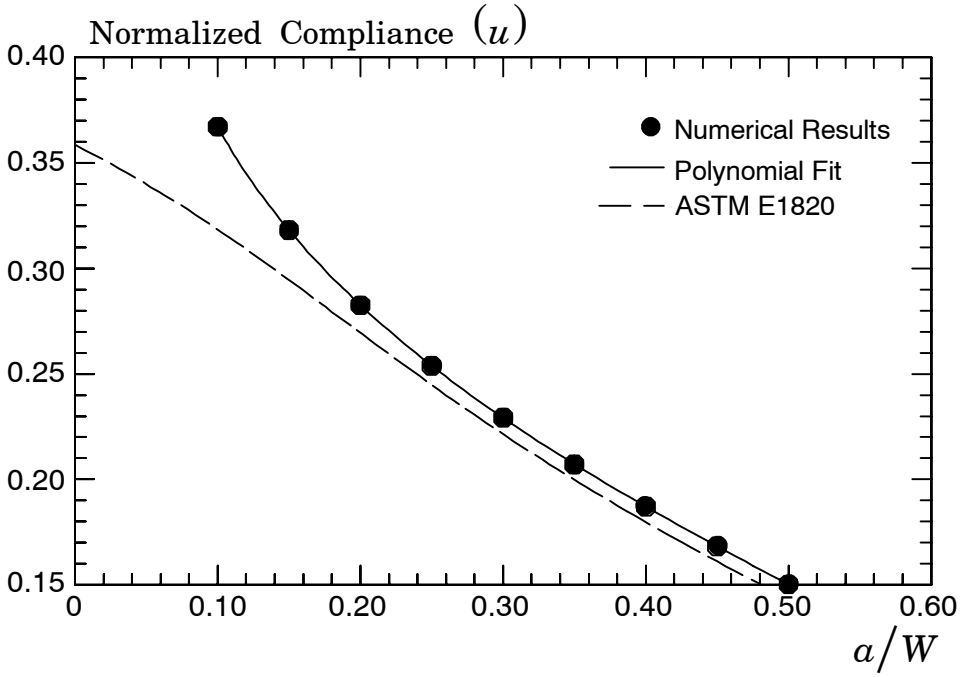

Figure 4. Normalized Compliance as a function of a/W for the analyzed SE(B) specimens.

4. Plastic η factor

The nonlinear finite elements analyses provide load, *CMOD* and *LLD* records to evaluate the η-factors upon which the J-integral can be determined. The J-value is computed at each load step using a domain integral method as described in previous section. The experimental estimation formula divides J into an elastic and plastic component given by

$$J = J_{el} + J_{pl} \tag{3}$$

The elastic J component, J_{el} is calculated from

$$J_{el} = \frac{K^2(1 - \nu^2)}{E} \tag{4}$$

where K is the elastic stress intensity factor for the specimen (Tada, 2000), E and n are the elastic modulus and Poisson's ratio respectively. The plastic J component is calculated using (Kirk and Dodds, 1992)

$$J_{pl} = \frac{(\eta_{LLD})}{Bb} A_{pl}^{lld} \tag{5}$$

or

$$J_{pl} = \frac{(\eta_{CMOD})}{Bb} A_{pl}^{CMOD} \tag{6}$$

where

A_{pl}^{LLD} : area under the load versus plastic load line displacement (LLD_{pl}) curve.

A_{pl}^{CMOD} : area under the load versus plastic crack mouth opening displacement ($CMOD_{pl}$) curve.

η_{CMOD} : the plastic η-factor at crack length a for *LLD* estimation.

η_{LLD} : the plastic η-factor at crack length a for *CMOD* estimation.

B : net specimen thickness.

b : the remaining ligament.

The η coefficients are then determined from the above expressions. The range of parameters considered in these analyses allows evaluation of the dependence of these coefficients on a/W and material properties.

The variation of coefficients η_{LLD} and η_{CMOD} with a/W and material properties determined from the finite elements results is summarized in Fig. 5 (a-b). Solutions for perfectly plastic materials (limit load solution), where available, are included in the figure. Each coefficient shows considerable variation with crack depth. The variation with material properties is small for both η_{LLD} and η_{CMOD}. The η_{LLD} factor is essentially independent of materials properties for $a/W < 0.3$ whereas the η_{CMOD} factor reveals a weak dependence on materials properties for $a/W > 0.3$. This behavior for the η_{CMOD} factor indicates that it is more applicable for measurement of fracture toughness in specimens whit shallow cracks. However, the effect of material properties is not significant for both cases.

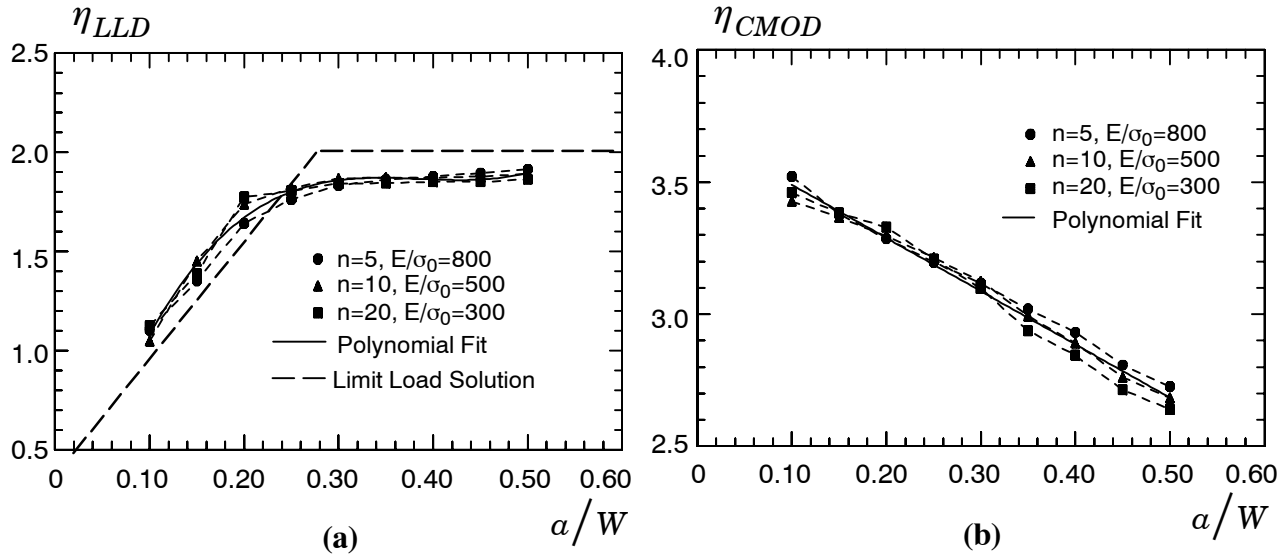

Figure 5. Plastic η-factors; (a) η_{LLD} for *LLD* measurement; (b) η_{CMOD} for *CMOD* measurement.

Another advantage of measuring J based upon the plastic area under the load vs. *CMOD* curve is associated with the actual compliance of the specimen. Because the measured *CMOD* relates directly to the specimen compliance, no further

correction is needed. In contrast, the measured *LLD* includes the specimen compliance with and without a crack. Since the compliance for the specimen without a crack is normally not evaluated, the plastic η_{LLD} can be inaccurate, particularly for shallow crack configurations (Saxena, 1998).

5. *J* Estimation Error

Figure 6 illustrates the variation of *J* with *LLD* and *CMOD* determined by finite element analysis for the SE(B) specimen with $a/W = 0.15$, n=10 and E/σ_0=500. This dependence of *J*-value on *LLD* and *CMOD* contrasts with that predicted by the *J* estimation procedures using η_{LLD} and η_{CMOD} coefficients calculated from the finite element results. *J* estimation using Eq. 6 (*CMOD*) matchs the finite element results more closely than Eq. 5 (*LLD*). Figure 7 shows the estimation error between *J* predicted using η method and *J* measured from finite elements. The error in *J* derived from the use of η_{LLD} is much larger than the error in *J* derived from η_{CMOD}.

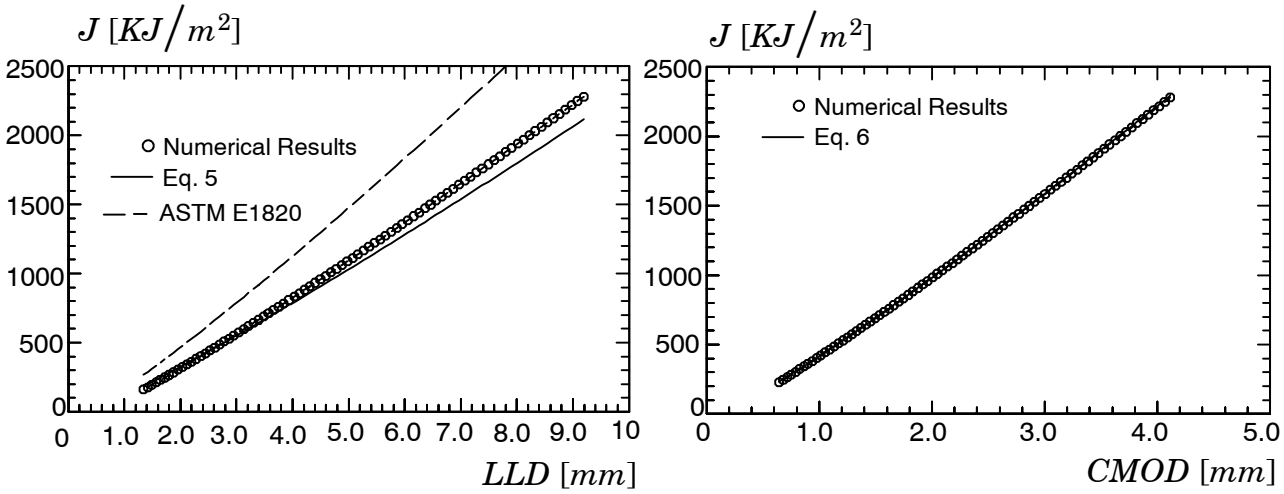

Figure 6. Variation of *J* with *LLD* and *CMOD* for the *SE(B)* specimen with $a/W = 0.15$, n=10 and E/σ_0=500 .

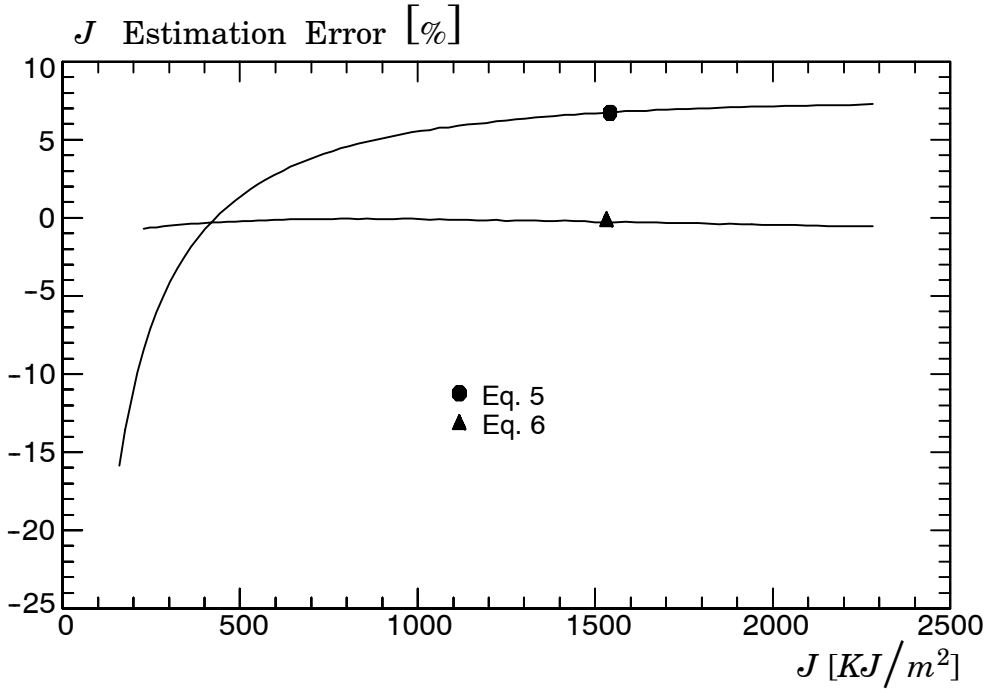

Figure 7. *J* estimation errors for the SE(B) specimen with $a/W = 0.15$, n=10 and E/σ_0=500.

6. *J* Estimation in a *J-R* curve test

In *J-R* curve tests, the *J* integral is also divided into elastic and plastic components given by

$$J = J_{el} + J_{pl} \tag{7}$$

The elastic *J* component, $J_{el,}$ is calculated as in a stationary crack analysis. The experimental estimation for the plastic component of *J* is evaluated incrementally. This portion of *J*-integral is calculated using (Anderson, 1995)

$$J_{pl(i)} = \left[J_{pl(i-1)} + \left(\frac{\eta_i}{b(i)} \right) \cdot \left(\frac{A_{pl(i)} - A_{pl(i-1)}}{B} \right) \right] \cdot \left[1 - \gamma_i \frac{\left(a_{(i)} - a_{(i-1)} \right)}{b_{(i-1)}} \right] \tag{8}$$

where

A_{pl} : area under the load versus plastic load line displacement (LLD_{pl}) or plastic crack mouth displacement ($CMOD_{pl}$) curve to crack increment *i*.

B : net specimen thickness.

η_i : the plastic η at crack length a_i.

b_i : the incremental remaining ligament.

W : the specimen width and

$$\gamma_i = \eta_i - 1 + \frac{1}{\eta_i} \frac{b_i}{W} \frac{d\eta_i}{d(b/W)} \tag{9}$$

As can be seen in Eq. (9), the evaluation of γ_i requires the first derivative of η_i with b/W which can be determined by (Anderson, 1995).

$$\frac{d\eta_i}{d(b/W)} = - \frac{d\eta_i}{d(a/W)} \tag{10}$$

Having obtained the values of η_{LLD} or η_{CMOD} for various a/W relations and interpolating for intermediate values, it is possible to determine their derivatives numerically. Therefore, γ_{LLD} or γ_{CMOD} are easily determined using Eq. (9) and the numerical derivative of η_{LLD} or η_{CMOD}. Figure 8 shows the variation of γ_{LLD} or γ_{CMOD} with a/W. It can be seen in Fig. 8-a that γ_{LLD} is approximately unity for $a/W > 0.3$ but changes to negative values for shorter cracks.

7. Concluding Remarks

Results from plane strain finite elements analyses are used to develop compliance equation and *J* estimation strategies which are more applicable for shallow crack SE(B) specimens. Crack depth to specimen width (a/W) ratios between 0.1 and 0.5 are modeled using a linear elastic material and a Ramber-Osgood material with strain hardening exponents, n = 5, 10 and 20 and elastic modulus to reference stress ratio (E/σ_0 = 800, 500 and 300) with E = 206 GPa and ν = 0.3.

The compliance equation agrees very well with the ASTM E1820 standard for crack sizes to specimen width ratios greater than 0.25 ($a/W > 0.25$). However, there is a marked difference for lower crack size to specimen width ratios ($a/W > 0.25$).

The estimation formulas for *J*-integral divide it into elastic and plastic components. The elastic component is determined by the linear elastic stress intensity factor, *K*. The formulas differ in evaluation of the plastic component. The techniques considered include estimation of *J* from plastic work based on load line displacement (*LLD*) and from plastic work based on crack mouth opening displacement (*CMOD*). This last technique provides the most accurate estimation procedure. The insensitivity of η_{CMOD} to material properties permits *J* estimation for any material with equal accuracy. Further, estimating *J* from *CMOD* rater than *LLD* eliminates the need to measure *LLD*, thus simplifying the test procedure.

8. Acknowledgements

This investigation was supported by the Scientific Foundation of the State of São Paulo (FAPESP) under grant 03/02735-6 and 04/07150-9 and by the National Council of Scientific and Technological Development - CNPq (Grant: PQ 300048/97-1).

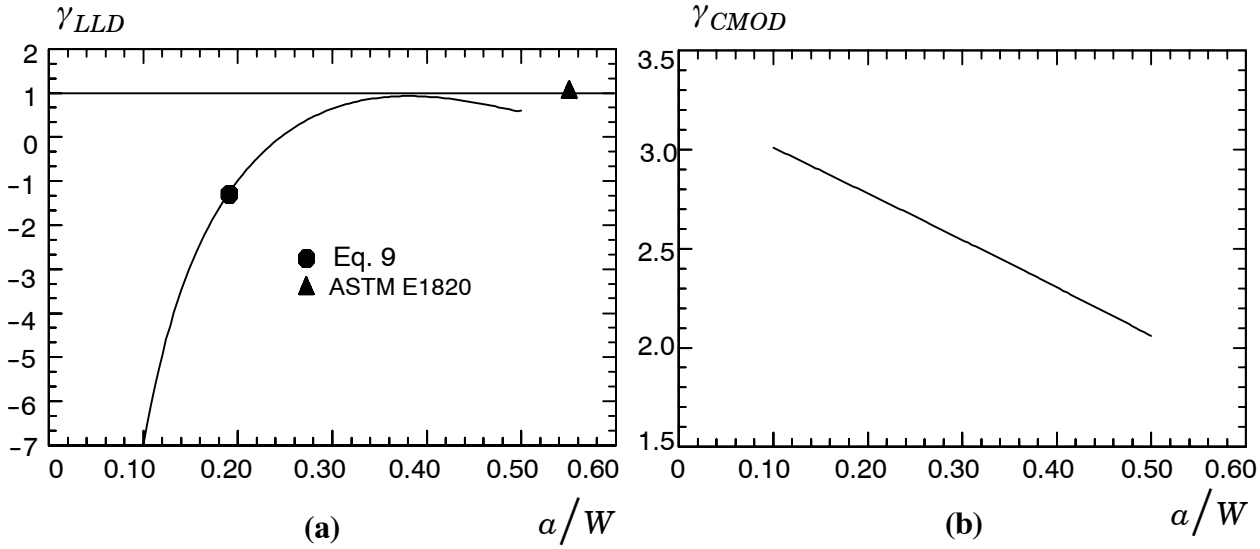

Figure 8. Variation of γ_{LLD} *and* γ_{CMOD} with *a*/*W*.

9. References

American Society for Testing and Materials, 2001, "Standard Test Method for Measurement of Fracture Toughness", ASTM E 1820-01, Philadelphia.

American Society for Testing and Materials, 1995, "Test Method for Determining J-R Curves", ASTM E 1152-95, Philadelphia.

American Society for Testing and Materials, 2002, "Standard Terminology Relating to Fatigue and Fracture Testing", ASTM E1823-96(2002), Philadelphia.

Anderson, T. L., 1995, "Fracture Mechanics: Fundaments and Applications", 2nd Edition, CRC Press, New York.

Moran, B., and Shih, C.F. "A General Treatment of Crack Tip Contour Integrals." *International Journal of Fracture,* 1987, (35):295-310.

Tada, H., Paris, P., C., Irwin, G., R., "The Stress Analysis of Cracks Handbook" - 3rd Edition, ASME, New York, 2000, pp. 47.

Kirk, T., M., and Dodds R., H., Jr., 1992, "J and CTOD Estimation Equation for Shallow Cracks in single edge Notch Bend Specimens", Civil Engineering Studies, Structural Research Series No. 565, Urbana-Champaign.

Koppenhoefer, K., Gullerud, A., Ruggieri, C., Dodds, R. and Healy, B., 1994, "WARP3D: Dynamic Nonlinear Analysis of Solids Using a Preconditioned Conjugate Gradient Software Architecture." Structural Research Series (SRS) 596. UILU-ENG-94-2017. University of Illinois at Urbana-Champaign.

Saxena, A., 1998, "Nonlinear Fracture Mechanic for Enineers", 1st Ed., CRC Press.

10. Responsibility notice

The authors are the only responsible for the printed material included in this paper.